CLM-P579

CLM-P579

UKAEA

Preprint

CONVECTIVE HEAT TRANSFER BENEATH HEATED PLATES BY HOLOGRAPHIC INTERFEROMETRY

T. A. DULLFORCE
R. A. FAW*
R. S. PECKOVER

CULHAM LABORATORY
Abingdon Oxfordshire

1979

CONVECTIVE HEAT TRANSFER BENEATH HEATED PLATES BY HOLOGRAPHIC INTERFEROMETRY

T A Dullforce
R A Faw*
R S Peckover

Culham Laboratory, Abingdon, Oxon. OX14 3DB, UK

ABSTRACT

Experimental studies of heat transfer from heated flat metal plates have been revived in recent years following early work in which thermocouple probes were the usual means of monitoring temperature profiles near the plate surface. For accurate results care had to be taken in positioning the probes and their finite size and trailing wires could disturb the convection pattern and hence the temperature field being measured. This paper briefly reviews the technique of live fringe holographic interferometry and describes its application to downward heat transfer from a horizontal square plate. The results are in good agreement with other average plate measurements.

Infinite fringe holograms were used to demonstrate the uniformity of temperature profiles across the plate (transverse to the laser beam direction) while the finite fringe technique was used to measure mean temperature profiles beneath the plate as a function of plate surface temperature. The predicted profiles derived from the analytical results of Singh, Birkebak and Drake are in good agreement with the experimental measurements while Nusselt numbers derived from the profiles are about 25% higher than the predicted values. Finite boundary layer thickness at the plate edges has been clearly demonstrated.

(Paper presented to 8th Experimental Thermodynamics Conference, University of Surrey, Guildford, 5-7 April, 1978)

* Nuclear Engineering Department,
Kansas State University,
Manhattan, Kansas, USA

August 1978

1 INTRODUCTION

After a long interval following the work of Weise[1], Kraus[2] and Saunders et al[3] Experimental studies of downward heat transfer by convection from horizontal surfaces have been revived in recent years. Table 1 summarises the latest work in which heat transfer to air and water from square and rectangular plates made from aluminium, brass and copper has been investigated. Like the early work, average Nusselt numbers were found to be proportional to the Rayleigh number to the power 0.2, with only slight variation in the proportionality constant.

With few exceptions the measurements were made with the help of thermocouples to monitor the temperature profiles in the air or water, from which local Nusselt numbers and boundary layer thicknesses could be derived. For accurate results with thermocouple techniques a lot of care has to be taken with the positioning of the thermocouples in order to know firstly the exact position of the probe junction and secondly that the probe and its trailing wires do not disturb convection and hence the temperature field being measured.

A much simpler and potentially very powerful technique exists in the form of laser holographic interferometry. Using the double exposure method only the changes that take place in the system, in our case those in the convecting medium, are recorded. Optical interference methods do not disturb the medium and they provide spatially continuous temperature profiles up to the heater surface, from which accurate temperature gradients and heat transfer rates can be obtained. The technique is very simple to execute, though not always so simple to analyse, and gives all the required information on a single record.

The purpose of this paper is to summarise one holographic method, to describe its application to the study of heat transfer beneath a heated square copper plate and to compare the results with previous measurements. The live-fringe holographic technique described in section 3 is covered in detail elsewhere[4] as are the full results of the experiments[5] given in section 5. Infinite-fringe holograms were used to demonstrate the uniformity of temperature profiles across the plate surface while the finite-fringe technique was used to measure mean temperature profiles as a function of plate surface temperature. We begin in section 2 with a brief summary of the holographic process.

2 THE HOLOGRAPHIC PROCESS

Holography, or photography by wavefront reconstruction imaging, discovered in 1948 by Gabor[6-9], is a technique whereby the light rays transmitted through or reflected from an object are recorded for reconstruction in space at a later time. The recording medium is usually a photographic plate which is exposed simultaneously to coherent light in a reference wave and in an object wave. Figure 1 illustrates the arrangement for transmission holography used in the present study and to which our discussion will be limited. The two waves form interference patterns in the plane of the photographic plate which are recorded as variations in optical density or refractive index of the developed plate. When the developed plate is illuminated by a coherent reconstruction wave, diffraction by the interference pattern leads to reconstruction of the original object wave. Three-dimensional images of the object are formed which may be examined in much the same way as the original object could have been examined.

We shall assume that the waves have uniform amplitude over the photographic plate surface which is in the x-y plane and that the object introduces phase changes only in the object wave. We can represent the time-averaged reference and object waves by the complex quantities

$$U_r(x,y) = u_r(x,y)\exp[j\phi_r(x,y)]$$

and

$$U_o(x,y) = u_o(x,y)\exp[j\phi_o(x,y)]$$

in which it is understood that only the real components have physical significance. u_r and u_o are the wave amplitudes and ϕ_r and ϕ_o the corresponding phases. The response of the plate emulsion depends on exposure which is proportional to the intensity of the incident light and given by :

$$I(x,y) = (U_r + U_o)(U_r^* + U_o^*)$$

in which U_r^* and U_o^* are complex conjugates.

A phase hologram (not to be confused with the term phase object) is one in which the photographic plate has been bleached during development to make it transparent. The plate introduces phase changes rather than amplitude changes in any transmitted light. When illuminated by a coherent reconstruction wave the transmitted wave is given by:

$$U_t(x,y) = t_f(x,y)U_c(x,y)$$

where $t_f(x,y)$ is a transmission factor equal to $1 + j\beta'I(x,y)$ for small values of $\beta'I(x,y)$. β' is a negative proportionality constant relating the change in refractive index in the developed plate (proportional to wave intensity I) to phase changes. If reconstruction is by the original reference wave, then $U_c = U_r$ and:

$$U_t = (1 + j\beta'u_r^2)U_r + j\beta'u_o^2U_r + j\beta'U_rU_rU_o^* + j\beta'u_r^2U_o \quad \ldots\ldots\ldots(1)$$

The transmitted wave therefore has four components. The first is just the reconstruction or reference wave attenuated by the factor $(1 + j\beta'u_r^2)$. The second contains extraneous information and can be neglected if the amplitude of the object wave is very much less than that of the reference wave, $u_r >> u_o$. The third and fourth terms contain information of interest in holography since they contain the original object wave and its conjugate. Term three results in a real image and the fourth term a virtual image positioned in the same place as the original object in relation to the re-positioned plate.

3 HOLOGRAPHIC INTERFEROMETRY OF PHASE OBJECTS

Holographic interferometry is a technique of double exposure holography. The photographic plate is exposed first with the object in some initial state and then after a change has been brought about in the object which results in refractive index changes between the exposures. The change in optical path length through the object between exposures results in interference fringes which may be viewed in the reconstruction of the doubly exposed object. The object wave may be thought of as made up of two components, the first, $U_{o1}(x,y)$, from the object in its initial state introduces phase variations $\phi(x,y)$ so that:

$$U_{o1} = u_o(x,y)\exp[j\phi(x,y)]$$

and the second component representing the object in its changed state giving rise to phase changes $\Delta\phi(x,y)$ superimposed on $\phi(x,y)$, ie:

$$U_{o2} = u_o(x,y)\exp[j(\phi + \Delta\phi)]$$

The total object wave is then:

$$U_o = U_{o1} + U_{o2} = u_o\exp(j\phi)[1 + \exp(j\Delta\phi)]$$

and the visual or photographic examination of the virtual image depends

on the intensity of the transmitted wave which is given by the last term of equation (1) as:

$$|j\beta' u_r^2 U_o|^2 = \beta'^2 u_r^4 |U_o|^2 = 4\beta'^2 u_r^4 u_o^2 \cos^2(\tfrac{1}{2}\Delta\phi)$$

In the image, brighter and darker regions called fringes, will appear as $\Delta\phi$ varies by multiples of 2π, with bright fringes (maximum intensity) occurring wherever $\Delta\phi = 2m\pi$ and dark fringes (minimum intensity) wherever $\Delta\phi = 2(m+\frac{1}{2})\pi$, with $m = 0, \pm1, \pm2 \ldots$. These fringes form an interferogram or contour map of the object, with fringes mapping contours of uniform phase change, similar to the infinite fringe setting of a Mach-Zender interferometer.

The phase change $\Delta\phi$ is related to the change in optical path length through the object, Δp, by $\lambda\Delta\phi = 2\pi\Delta p = 2\pi\Delta(ln)$ where λ is the wavelength used, 1 is the linear path and n the medium refractive index. In the experiments below 1 was constant so that phase changes were due only to changes in n. Between adjacent light or dark fringes ($m = 1$) $\Delta\phi = 2\pi$ from which $1\Delta n = \lambda$. Since Δn is related to temperature change ΔT, the spacing of the fringes may then be expressed in terms of ΔT, thus:

$$1\Delta T(dn/dT) \sim \lambda$$

and the fringes map contours of uniform temperature.

Variations in optical path length are clearly mapped but there are disadvantages to the infinite-fringe technique. It is difficult to determine whether adjacent fringes correspond to increases or decreases in optical path length and a reference point of known path length is difficult to identify. Also, fringe spacing is proportional to ΔT and fringes can be very closely spaced, perhaps non-resolvably, in regions of large temperature gradients.

In the finite-fringe technique a uniform variation in phase is superimposed on the object wave during exposure of the disturbed object. This can be done in several ways. Reference 4 gives the analysis for the case of a thin-walled wedge containing a gas of refractive index n_g relative to air introduced into the object beam. The result is a pattern of straight, parallel and equally spaced fringes which become distorted when the object is stressed. Phase changes may then be determined by comparing the fringe patterns in the distorted and

undistorted regions of the image. Of course, undistorted regions must be present but the finite-fringe technique offers considerably more flexibility than the infinite-fringe technique. The spacing of the finite-fringes can be controlled, by for example adjusting the gas pressure in the wedge.

A slight variation in the double exposure technique described above is given by first preparing and processing a hologram of the object in its quiescent state and then illuminating it with the original reference wave and the object wave of the perturbed object. Time variations in the refractive index field result in moving fringes giving 'real-time' or 'live-fringe' interferometry. Conventional photography of the moving image can then be made. This technique, used in the experiments below, requires extreme care in the re-positioning of the hologram plate to avoid fringes due to misalignment.

4 EXPERIMENTAL APPARATUS AND PROCEDURE

The overall arrangement of the apparatus is shown in figure 1 and described in detail in reference 5. The beam from a continuous wave argon-ion laser with intra-cavity etalon and operating at 500 mW was elevated by a pair of beam positioning mirrors to about 25 cm above a vibration isolated granite bench. After passing through a shutter, the beam was divided into two equal components (reference and object beams) by a beam splitting cube. The reference beam was expanded by a 20 x microscope objective and filtered by an 11μm dia.pin-hole located 55 cm from the hologram plate and the expanded beam struck the plate at about 45°. The object beam was expanded and filtered by a 20 x objective and 25μm pin-hole located 180 cm from a ground glass diffuser plate 20 cm wide and 25 cm high, parallel to and 30 cm from the hologram plate. The heat transfer plate was located between the diffuser and hologram plates with its horizontal surface about 30 cm above the bench. It was centred on and aligned with the axis of the object beam.

The heat transfer plate was a 16 cm square copper plate 1.25 cm thick. Sixteen thermocouples were located in one sector of the plate in wells drilled to within 1 mm of the plate surface. The plate was heated by four independent nichrome heating elements encased in ceramic insulating tubes recessed into grooves in an insulating backing plate 15.8 cm square (slightly smaller than the copper plate so as not to disturb flow around the edge of the heat transfer plate). The elements

were individually powered through variable transformers connected to the 240V 50 Hz mains supply and the plate temperature was easily held uniform to within 0.5 K.

With the heat transfer test plate at ambient temperature a hologram plate was exposed for 0.25 s, processed (including bleaching) and carefully re-positioned in its holder where it was again illuminated by the object and reference beams. A virtual holographic image of the test plate then appeared superimposed on the actual plate. A system of parallel interference fringes was then introduced by adjusting slightly the angle of incidence of the reference beam. This was the finite-fringe setting illustrated in figure 2. The reference beam angle undisturbed produced the infinite fringe setting.

The plate temperature was then increased. Convective cooling of the plate caused density changes and corresponding refractive index changes in the air. These caused optical interference leading to distortion of the finite-fringes, or the appearance of fringes in the infinite-fringe setting.

Interference patterns were photographed with a 35 mm camera and a 55 mm lens placed about 50 cm from the hologram plate. Exposures were made with a total laser beam power of 1 W with a 50% filter in the object beam. Typical exposures were 0.125 s at f/22 using Ilford HP4 film rated at 400-650 ASA.

5 EXPERIMENTAL RESULTS

Figures 2 and 3 show typical finite-fringe interferograms for plate temperatures of 296 K (ambient or T_∞) and 336 K respectively. The fringe patterns intersect the surface of the heater plate, the edge of which is visible. Also visible is a line (shadow) marking the centre of the plate. The line and edge, 8 cm apart, provided a scale factor for measurements from the photographs.

Figure 4 illustrates the interpretation of the fringe shifts. One particular centrally located dark fringe is shown with projections of the adjacent fringes from the region of the photograph in which they are straight and parallel. Adjacent pairs of dark fringes result from a change in optical path of one wavelength, λ = 514.5 nm, of the light. In figure 4 the intersection marked m = 2 is a point distance y beneath the plate at which the temperature change in the

air caused a change in optical path length of 2λ. The intersection at the plate surface may be a non-integral number m_w.

Using the Gladstone-Dale law ($n-1 = K\rho$) connecting the refractive index of a gas with its density, ρ, and the ideal gas law, the variation of n with T may be derived as:

$$\frac{dn}{dT} = - \frac{KP}{RT^2}$$

where K is the Gladstone-Dale constant, P the pressure and R the gas law constant. If the temperature change corresponding to m fringe shifts is written $\theta = (T - T_\infty)$ where T_∞ is the ambient air temperature far removed from the thermally disturbed region near the plate surface, it follows that:

$$T^{-1} = T_\infty^{-1} - (mR\lambda/KP1) \quad \ldots\ldots\ldots\ldots\ldots\ldots (2)$$

The changes monitored interferometrically are averaged over the beam path length and were made at the plate centre line. Thus,

$\overline{\theta}(y) = [\overline{T}(y) - T_\infty]$ and, since m_w fringe shifts correspond to $\theta_w = (T_w - T_\infty)$, the averaged temperature change, $\overline{\theta}(y)$, may be computed from equation (2) in terms of the non-dimensional parameter $\psi = \overline{\theta}(y)/\theta_w$ as:

$$\psi = \left[1 + \frac{T_w}{T_\infty}\left(\frac{m_w}{m} - 1\right)\right]^{-1}$$

Values of y were measured corresponding to the various fringe orders and the value of $d\overline{\theta}/dy$ determined graphically from which the average Nusselt number, $\overline{Nu}$, and the boundary layer thickness, δ_o, could be calculated using:

$$\overline{Nu} = - \frac{a}{\theta_w} \frac{d\theta_w(o)}{dy}$$

$$\delta_o = -2\theta_w / \frac{d\overline{\theta}_w(o)}{dy}$$

With physical values evaluated at a reference temperature $T_{ref} = T_w - 0.38\theta_w$ Rayleigh numbers were calculated from:

$$Ra = g\beta a^3 \theta_w / \alpha\nu$$

where 2a is the length of the plate sides, β the coefficient of thermal expansion, α the thermal diffusivity and ν the kinematic viscosity. Figure 5 shows ψ plotted against the non-dimensional distance $v = y/\delta_o$ for four plate surface temperatures, while figure 6 gives a plot of $\overline{Nu}$ against Rayleigh number.

Also shown in figures 5 and 6 are theoretical curves based on the analytic results of Singh et al[9]. The predicted values of ψ (v) agree quite well with the experimental results, while the predicted values of $\overline{Nu}$ are about 25% lower than the experimental values. The measurements, however, are in excellent agreement with the measurements of Restrepo and Glicksman [10] in air and by Birkebak and Abdulkadir[11] in water.

Infinite-fringe interferograms showed that the boundary layer temperature had little lateral variation near the centre line of the heated plate, while finite-fringe photographs centred on the plate edge for θ_w = 33 K showed a finite boundary layer thickness, contrary to some predictions, at the plate edge.

Acknowledgement

This work was supported by the UK Safety and Reliability Directorate, Culcheth, whose support is gratefully acknowledged.

References

1 Weise, R., Wärmeübergang durch freie Konvektion an quadratishen Platten, Forsh. auf Gebiet Ing., 6, 281-292 (1935)

2 Kraus, W., "Temperatur-und Geschwindigkeitsfeld bei freier Konvektion um eine waagerechte quadratische Platte", Physik Zeits, 4, 126-150 (1940)

3 Saunders, O.A., Fishendon, M. and Mansion, H.D."Some measurements of convection by an optical method", Engineering, 483-485 (May 1935)

4 Faw, R.E. and Dullforce, T.A., "Holographic interferometry: principles and procedures", Report CLM-RR/S2/19, UKAEA, Culham Laboratory, (1977)

5 Faw, R.E. and Dullforce, T.A., "Convective heat transfer beneath a heated horizontal plate", Report CLM-RR/S2/24, UKAEA, Culham Laboratory, (1977)

6 Gabor, D., "A new microscope principle", Nature, May 15 1948.

7 Gabor, D., "Microscopy by reconstructed wavefronts", Proc. Roy. Soc., A197, 454-487, (1949)

8 Gabor, D., "Microscopy by reconstructed wavefronts: II", Proc. Phys. Soc., 64, 450-469, (1951)

9 Singh, S.N., Birkebak, R.C. and Drake, R.M., "Laminar free convection heat transfer from downward facing horizontal surfaces of finite dimensions", Progr. in Heat and Mass Transfer, vol. II, Pergamon Press, 87-98, (1969)

10 Restrepo, F. and Glicksman, L.R., "The effect of edge conditions on natural convection from a horizontal plate", Int. J. Heat Mass Transfer, 17, 135-142, (1974)

11 Birkebak, R.C. and Abdulkadir A, "Heat transfer by natural convection from the lower side of finite horizontal, heated surface", Fourth International Heat Transfer Conference, Paris, vol.4, Paper NC2.2, (1970)

12 Fujii, T. and Imura, H., "Natural convection heat transfer from a plate with arbitrary inclination", Int. J. Heat Mass Transfer, 15, (1972)

13 Aihara, T., Yamada, Y. and Endo, S., "Free convection along the downward facing surface of a heated horizontal plate", Int. J. Heat Mass Transfer, 15, (1972)

TABLE 1 RECENT EXPERIMENTAL RESULTS

Birkebak & Abdulkadir 1970 ref.11	Square aluminium plate, sides cooled to ambient temperature. Thermocouple probes.	Temp. profile and local Nusselt number agree with Singh et al[9] for square plate. $\overline{Nu} = 0.68\ Ra^{0.2}$
Fujii and Imura 1972 ref.12	Rectangular brass plates in water. Shorter sides insulated.	In range $10^6 < Ra < 10^{11}$ $\overline{Nu} = 0.58\ Ra^{0.2}$ Boundary flow laminar
Aihara, Yamada and Endo 1972 ref.13	Brass plates in air, shorter sides insulated. Thermocouple probes.	Temp. profile agrees with Singh et al[9] for infinite strip. $\frac{\theta(z,y)}{\theta_w} = \left[1+\frac{y}{\delta(z)}\right]\ \left[1-\frac{y}{\delta(z)}\right]^3$
Restrepo and Glicksman 1974 ref.10	Square copper plate. Insulated sides at surface temp. or cooled to ambient. Thermocouple probes.	Boundary layer thickness greater with cooled sides. With heated sides: $\overline{Nu} = 0.68\ Ra^{0.2}$

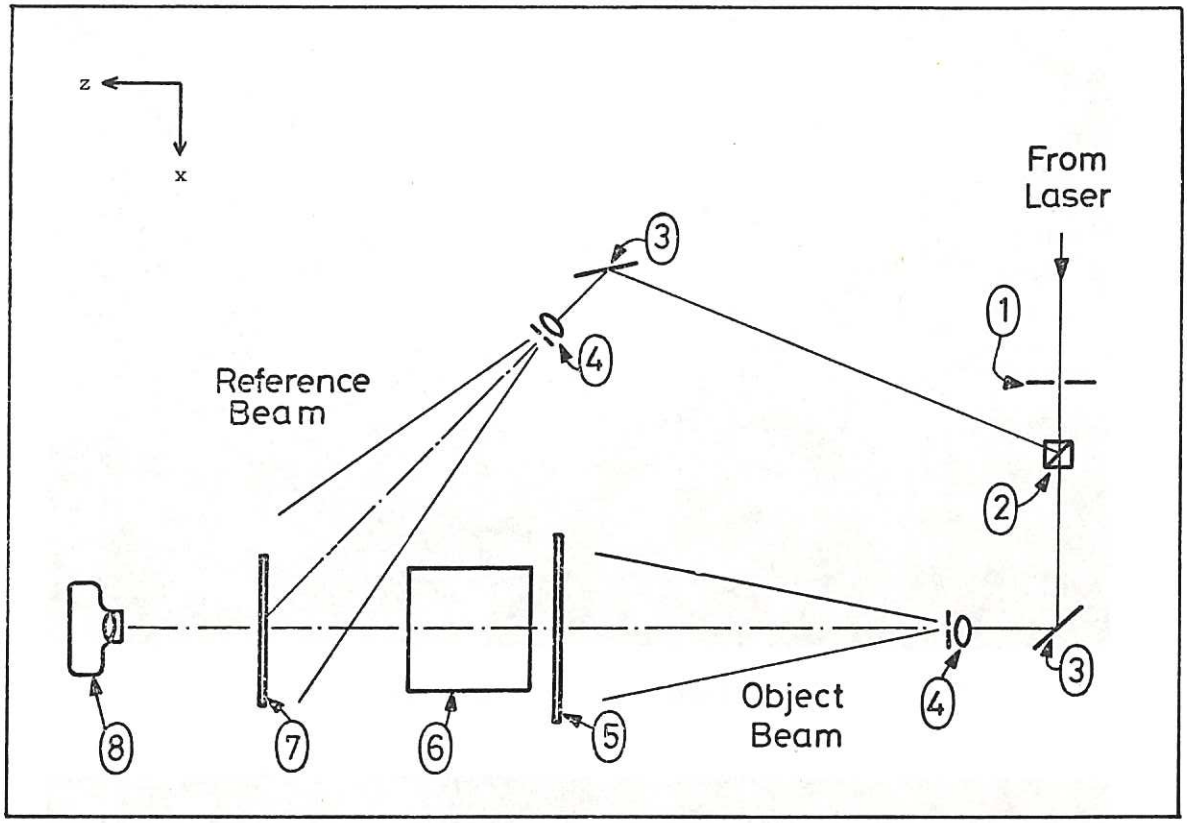

Fig.1 Schematic representation of apparatus for holographic interferometry: (1) shutter; (2) beam splitter; (3) mirrors; (4) beam expanders and pinholes (spatial filters); (5) ground-glass diffuser plate; (6) heat-transfer test cell; (7) hologram plate and (8) camera.

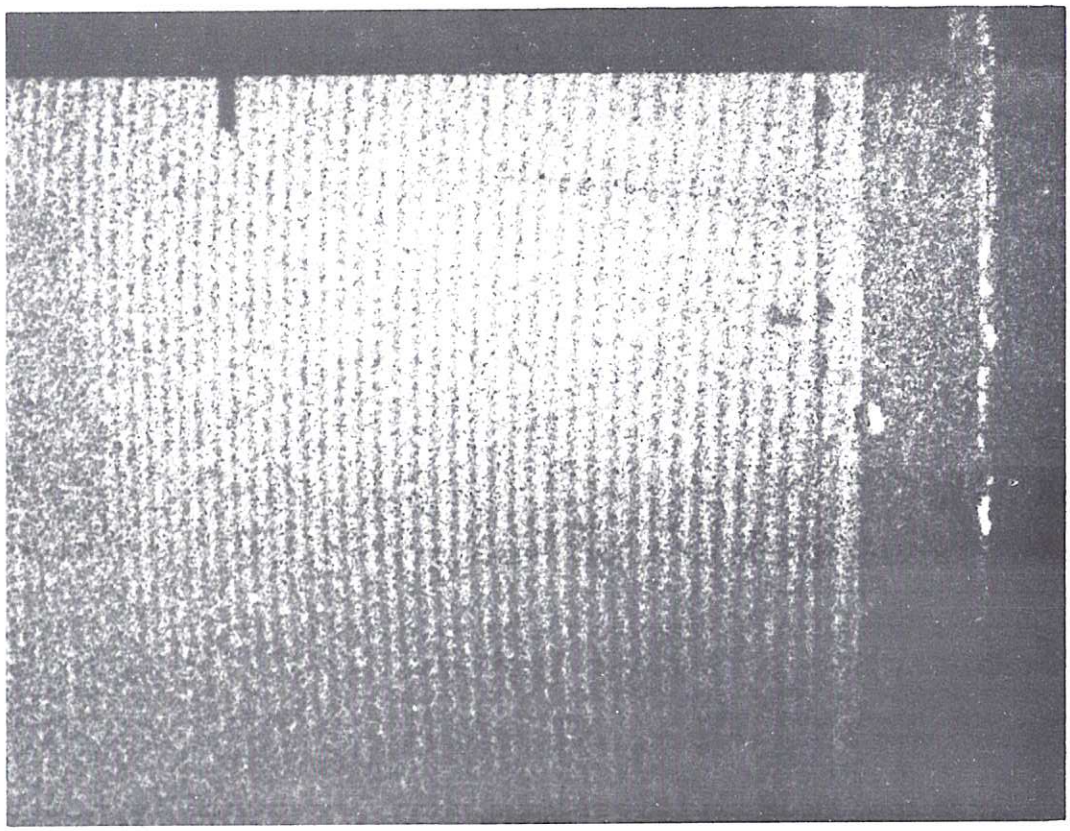

Fig.2 Finite fringes, $T_w = T_\infty = 296^\circ K$.

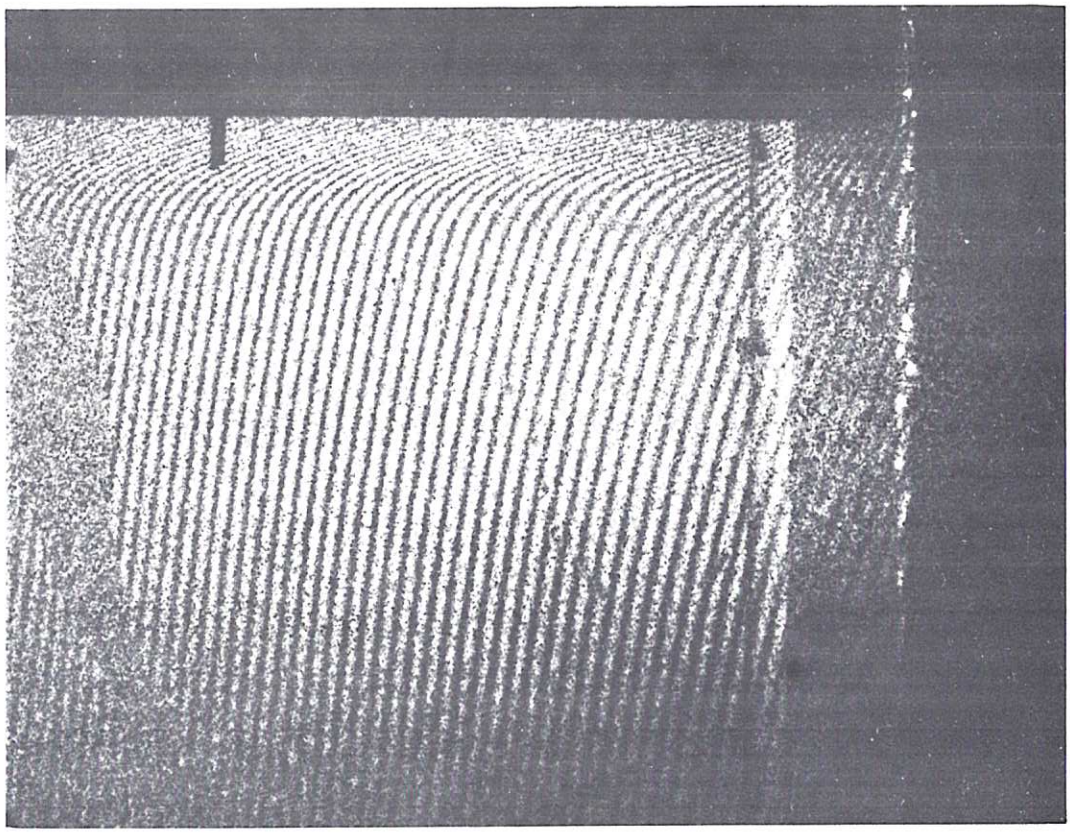

Fig.3 Finite fringes, $T_w = 336^\circ K$, $T_\infty = 296^\circ K$.

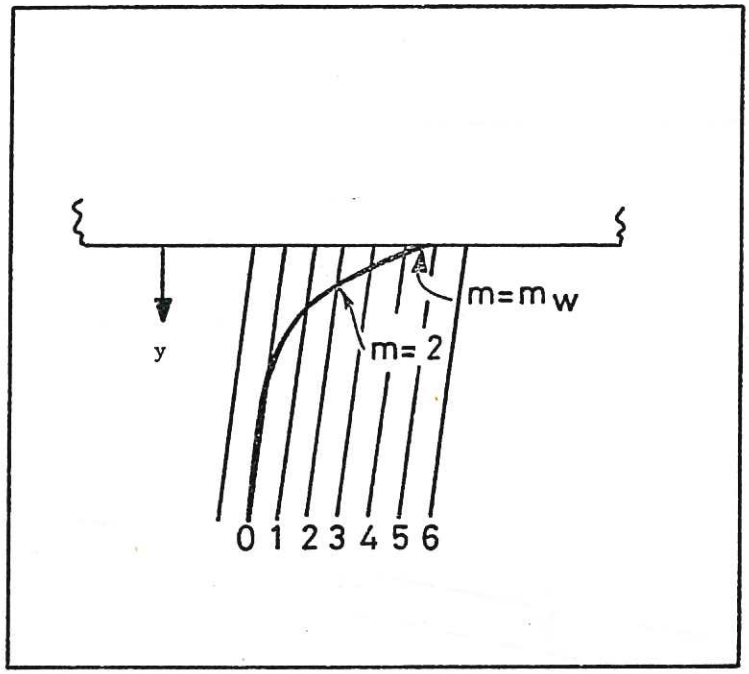

Fig.4 Interpretation of interference patterns.

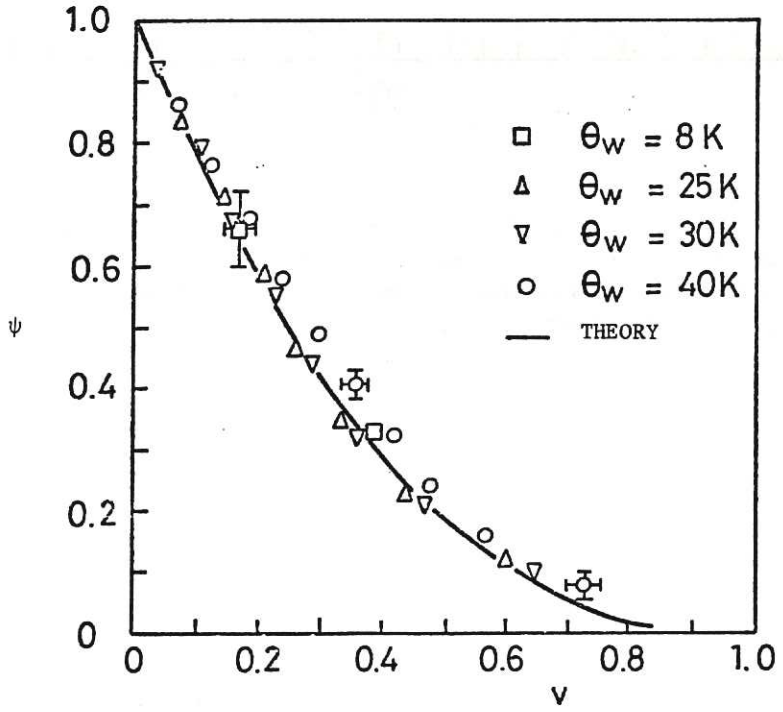

Fig.5 Composite results for $\psi = \overline{\theta}/\theta w$ vs. $v = z/\delta_o$. Only representative error bars are shown.

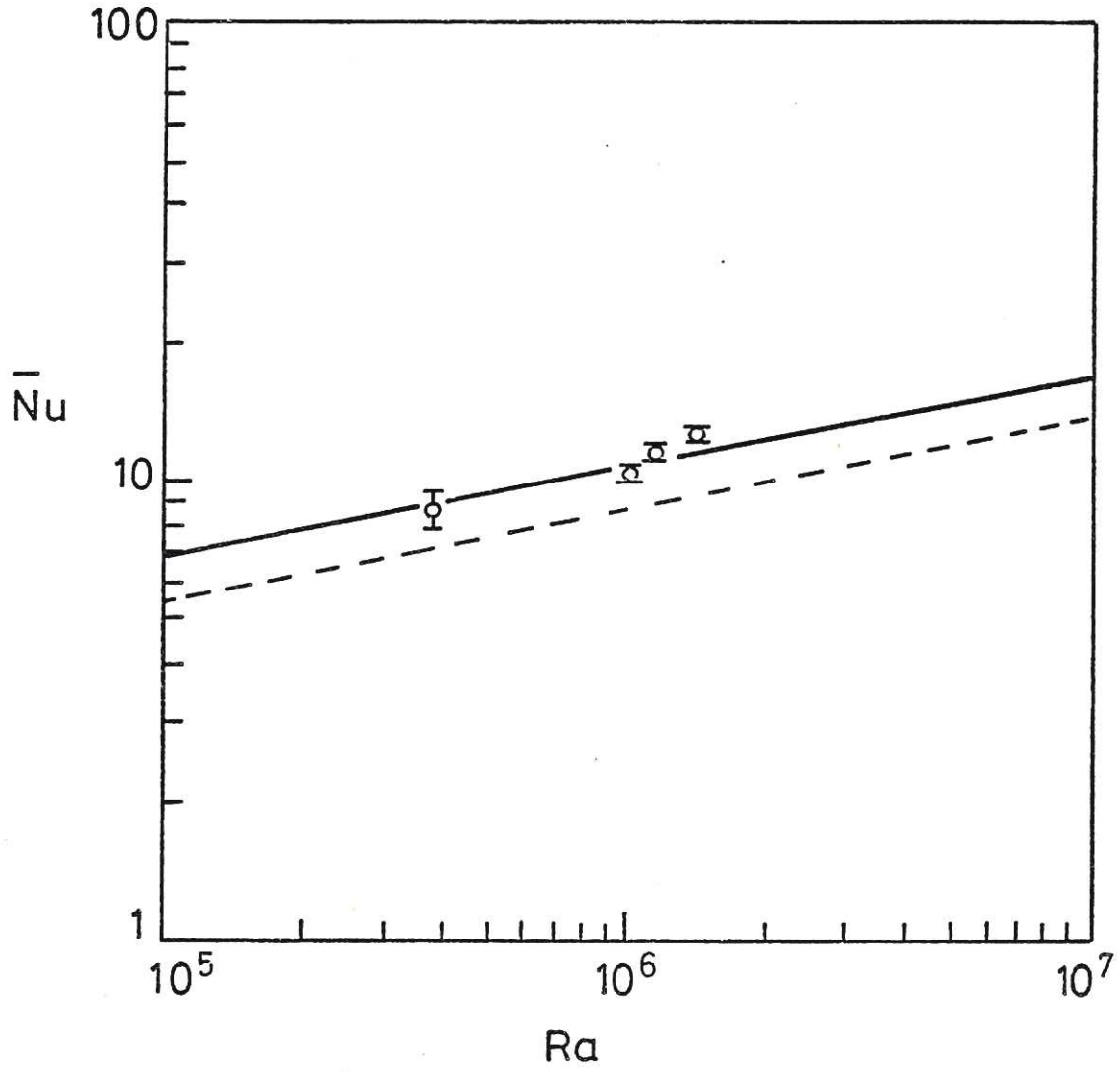

Fig.6 Nusselt number vs. Rayleigh number. Solid line: experimental results of Birkebak and Abdulkadir[11] and Restrepo and Clicksman[10] for averages over square plates. Broken line: based on analysis by Singh, Birkebak and Drake[9].